J. Marine Sci. Appl. (2015) 14: 366-375
DOI: 10.1007/s11804-015-1325-7

Wave Interaction with Dual Circular Porous Plates

Arpita Mondal and R. Gayen*

Department of Mathematics, Indian Institute of Technology, Kharagpur, 721302, India

Abstract: In this paper we have investigated the reflection and the transmission of a system of two symmetric circular-arc-shaped thin porous plates submerged in deep water within the context of linear theory. The hypersingular integral equation technique has been used to analyze the problem mathematically. The integral equations are formulated by applying Green's integral theorem to the fundamental potential function and the scattered potential function into a suitable fluid region, and then using the boundary condition on the porous plate surface. These are solved approximately using an expansion-cum-collocation method where the behaviour of the potential functions at the tips of the plates have been used. This method ultimately produces a very good numerical approximation for the reflection and the transmission coefficients and hydrodynamic force components. The numerical results are depicted graphically against the wave number for a variety of layouts of the arc. Some results are compared with known results for similar configurations of dual rigid plate systems available in the literature with good agreement.

Keywords: water wave scattering; circular-arc-shaped plates; hypersingular integral equation; Green's integral theorem; reflection coefficient; energy identity; hydrodynamic force

Article ID: 1671-9433(2015)04-0366-10

1 Introduction

Interaction of water waves with the obstacles of various geometrical shapes and sizes has been widely studied in the modern literature, due to the huge number of applications in the modeling of breakwaters that are constructed mainly to protect sheltered areas such as harbours, marinas, *etc*. from the impact of rough seas. An account of the detailed literature in the field of wave scattering problems involving barriers can be found in Mandal and Chakrabarti (2000). Ursell (1947) obtained the first rigorous mathematical analysis for an obstacle in the form of a partially immersed thin vertical plate, or a submerged thin vertical barrier extending infinitely downwards, by using an integral equation formulation. Since then a large number of research papers have been published by various researchers in this fascinating area of applied mathematics. Evans (1970) used the complex variable technique to investigate the wave scattering problem of a vertical plate completely submerged in deep water. Applying a reduction procedure and an integral equation formulation, Porter (1972) solved the problem of wave transmission through a small gap of arbitrary width.

However if the plate is curved, it is not possible to obtain an explicit analytical solution for the related water wave scattering problems. For such problems, some approximation techniques are used to obtain numerical values for the things of physical interest, namely the reflection and the transmission coefficients. Parsons and Martin (1994) investigated water wave scattering by a submerged thin curved plate, convex upwards and symmetric about a vertical line passing through the centre of the arc, and a surface piercing inclined plate in deep water, using the hypersingular integral equation technique. Subsequently, McIver and Urka (1995) used multipole potentials and a matching procedure to obtain numerical results for the reflection coefficient for a circular arc shaped plate submerged in deep water. Their motivation was to compare the reflective properties between a circular arc shaped plate and a submerged full circle, for assessing the acceptability of using circular plates in the construction of a water wave lens that might be helpful in focusing waves prior to extracting energy from them. Kanoria and Mandal (2002) investigated the problem of wave scattering by a submerged thin circular-arc-shaped plate, not necessarily symmetric about the vertical through its centre, submerged in infinitely deep water using a hypersingular integral equation technique.

Water wave scattering problems involving double or multiple barriers are fairly common in the modern literature. Seminal investigations involving the problems of scattering of water waves by two thin and impermeable vertical barriers of different configurations were performed by Levine and Rodemich (1958), Jarvis (1971), Newman (1974), Das *et al*. (1997), Neelamani and Vedagiri (2002), De *et al*. (2009; 2010) applying various mathematical techniques. In the field of porous structures, the scattering of water waves by double or multiple porous structures are somewhat rarely available in the literature. Research articles involving double permeable structures can be found in Twu and Lin (1991); Losada *et al*. (1992); Isaacson *et al*. (1999); Koraim *et al*. (2011). The response of double curved barriers towards water wave interaction can only be found in Mandal and Gayen (2002). They used the hypersingular integral equation technique as described in Parsons and Martin

Received date: 2015-02-10.
Accepted date: 2015-05-15.
Foundation item: Partially Supported by the Department of Science and Technology Through a Research Grant to RG (No. SR/FTP/MS-020/2010).
***Corresponding author Email:** rupanwita@maths.iitkgp.ernet.in

© Harbin Engineering University and Springer-Verlag Berlin Heidelberg 2015

(1994) for investigating the scattering of water waves by two symmetric circular-arc-shaped rigid plates submerged in deep water. This use of hypersingular integral equations is most acceptable in the sense that it can be adapted to study water-wave-interaction problems involving obstacles in the form of thin curved plates having any geometrical shape. The only limitation of this methodology is that it might not be directly extended to the case of a plate with finite width. However, in that case the problem can be formulated in terms of the discontinuity in the displacement across a two-dimensional cross section of the plate. The rectangular cross section may further be transformed into a circular disc by some conformal mapping. This will produce a two-dimensional hypersingular integral equation of order three which can be solved using the Fourier-Gegenbauer expansion method.

Here we have extended the work of Mandal and Gayen (2002) in the case of porous structures, namely double circular-arc-shaped permeable plates, placed symmetrically about the *y*-axis in deep water. Earlier Lu and He (1989) analyzed the phenomenon of the reflection and transmission of water waves by a thin curved permeable barrier and showed that a well planned curved porous plate was very effective in trapping waves within a large frequency range.

This paper deals with a water wave scattering problem involving two symmetric circular arc shaped thin porous plates submerged in deep water. Submerged plates are used to protect the shore-ward area of the breakwater from the hazards of rough seas by diminishing the effects of incoming waves. Such structures are effective as they allow the free exchange of water mass through them so that the water pollution in the sheltered area is minimized. The submerged structures are also capable of absorbing some wave energy, they break up waves and thus control shore erosion.

Here the curved plates are mounted so that the centers of the circular arcs are placed along a horizontal line joining the centers of two circles. The circular arcs are symmetric about the *y*-axis. Utilizing the geometrical symmetry of the plates, the velocity potential for the fluid motion when a train of regular, small amplitude surface water waves are striking the plates, is divided into two parts, namely the symmetric and the anti-symmetric potential functions. Then appropriate use of Green's integral theorem to the suitable functions in the fluid region, followed by utilization of the boundary condition on the porous plate surfaces produces two hypersingular integral equations of the second kind involving discontinuities of the symmetric, and the anti-symmetric potential functions across one of the two porous plates. These hypersingular integral equations are then solved numerically using an expansion-cum-collocation method, where the unknown discontinuities of the potential functions across the plates are approximated using two finite series involving Chebyshev polynomials of the second kind. The zeros of the Chebyshev polynomials are used as the collocation points. The numerical estimates for the reflection and transmission coefficients and the hydrodynamic forces are then computed using the solutions of the hypersingular integral equations. The numerical results for the reflection and transmission coefficients for a set of values of the depth parameters, arc lengths of the plates, and separation length between the centers of the circles whose arcs indicate the positions of the plates, are plotted graphically against the wave number in a number of figures. Some results are compared with the results of Mandal and Gayen (2002) for two circular arc shaped rigid plates submerged in deep water by taking the zero value of the porosity parameter. A very good agreement has been found in each case. Some new results are also provided here showing the effect of porosity in the reflection and transmission of the waves by a system of two curved porous plates. A significant result is achieved by taking two very closely spaced semi-circular arc shaped plates. Such a configuration serves as the cross section of a horizontal circular cylinder. It is observed that in this case there is almost no reflection. Ursell (1950) and Mandal and Gayen (2002) showed that a rigid horizontal circular cylinder offers no hindrance to incoming waves. Comparison of our results with those in Mandal and Gayen (2002) shows that a horizontal porous circular cylinder is more transparent to the incoming waves than the rigid one.

2 Mathematical formulation

We choose a two-dimensional Cartesian co-ordinate system with the *y*-axis directed vertically downwards passing through the midpoint of the line joining the centers of the circular arcs. The *xz*-plane denotes the position of the undisturbed free surface. The fluid occupies the region $0 < y < \infty, -\infty < x < \infty$. Two circular arc shaped thin porous plates $\Gamma_i (i = 1, 2)$ are situated inside the water as given in the Fig. 1. The vertical section of each of the plates are in the form of an arc of a circle of radius b with their centers at $(\pm a, d + b)$. The plates are considered to be infinitely long in the *z*-direction and we take a vertical cross-section in the *xy*-plane. Thus the motion is taken to be two-dimensional in the *xy*-plane.

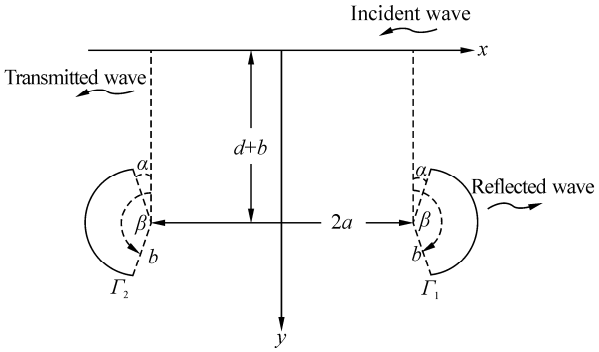

Fig. 1 Geometry of the dual porous plates

The upper and the lower end points of each circular arc make angles α and β respectively with the upward

vertical. The parameters a, b, α and β will always satisfy the identity

$$a \geq \max(-b\sin\alpha, -b\sin\beta) \tag{1}$$

Considering linear theory, incompressible and inviscid fluid, and irrotational motion, a train of surface water waves coming from the direction of positive infinity can be described by the potential function $\mathrm{Re}\{\phi_0(x,y)\mathrm{e}^{-\mathrm{i}\sigma t'}\}$, where t' is the time, σ is the frequency and

$$\phi_0(x,y) = 2\mathrm{e}^{-Ky-\mathrm{i}K(x-a)} \tag{2}$$

with $K=\dfrac{\sigma^2}{g}$, g being the acceleration due to gravity. Let the resulting motion in the fluid be expressed by the potential function (actual) $\mathrm{Re}\left\{\dfrac{g^2}{\sigma^3}\phi(x,y)\mathrm{e}^{-\mathrm{i}\sigma t'}\right\}$. Then $\phi(x,y)$ satisfies

$$\nabla^2\phi = 0 \text{ in the fluid region} \tag{3}$$

where ∇^2 denotes the two dimensional Laplace operator, along with the free surface condition

$$K\phi + \frac{\partial\phi}{\partial y} = 0 \quad \text{on} \quad y=0 \tag{4}$$

and the condition on the porous plate surface as given by

$$\frac{\partial\phi}{\partial n}\left(\Gamma_i^+\right) = \frac{\partial\phi}{\partial n}\left(\Gamma_i^-\right) = -\mathrm{i}KG[\phi](s_i) \tag{5}$$

where $[\phi](s_i) = \phi\left(\Gamma_i^+\right) - \phi\left(\Gamma_i^-\right)$, $\Gamma_i^{\pm}$ denote the right and the left hand sides of the plate Γ_i and s_i is any point on Γ_i, i=1, 2. Here $\dfrac{\partial}{\partial n}$ denotes the normal derivative at a point on Γ_i and G is the porous-effect-parameter defined by Yu and Chwang (1994) as

$$G = G_r + \mathrm{i}G_i = \frac{\gamma\left(f^* + \mathrm{i}S\right)}{kd_1\left(f^{*2} + S^2\right)}$$

where γ is the porosity; f^* is the resistance force coefficient; S is the inertial force coefficient and d_1 is the thickness of the porous medium. The velocity potential ϕ also satisfies the tip condition given by

$$r^{1/2}\nabla\phi \text{ is bounded as } r \to 0 \tag{6}$$

where r is the distance of any fluid particle from either of the submerged tips of Γ_i, i=1, 2, the bottom condition as given by

$$\nabla\phi \to 0 \text{ as } y \to \infty \tag{7}$$

$\phi(x,y)$ has asymptotic behavior

$$\phi(x,y) \to \begin{cases} \phi_0(x,y) + R\phi_0(-x,y) & \text{as } x \to \infty \\ T\phi_0(x,y) & \text{as } x \to -\infty \end{cases} \tag{8}$$

where R and T denote the reflection and transmission coefficients respectively, and are to be obtained.

3 Method of solution

Due to the geometrical symmetry about x=0, the velocity potential $\phi(x,y)$ can be divided into two parts namely the symmetric and the anti-symmetric parts $\phi^s(x,y)$ and $\phi^a(x,y)$ so that

$$\phi(x,y) = \phi^s(x,y) + \phi^a(x,y) \tag{9}$$

where

$$\phi^s(x,y) = \phi^s(-x,y), \quad \phi^a(x,y) = -\phi^a(-x,y) \tag{10}$$

Therefore we can confine our analysis to the region $x \geq 0$ only. Then $\phi^{s,a}(x,y)$ will satisfy the Eqs. (3)–(4), (6)–(7) together with

$$\frac{\partial\phi^s(0,y)}{\partial x} = 0, \ \phi^a(0,y) = 0, \ y > 0 \tag{11}$$

and

$$\frac{\partial\phi^{s,a}}{\partial n}\left(\Gamma_1^+\right) = \frac{\partial\phi^{s,a}}{\partial n}\left(\Gamma_1^-\right) = -\mathrm{i}KG\left[\phi^{s,a}\right](s_1) \text{ on } \Gamma_1 \tag{12}$$

Let the behaviour of $\phi^{s,a}(x,y)$ for large x be expressed by

$$\phi^{s,a}(x,y) \sim \mathrm{e}^{-Ky}\left\{\mathrm{e}^{-\mathrm{i}K(x-a)} + R^{s,a}\mathrm{e}^{\mathrm{i}K(x-a)}\right\} \text{ as } x \to \infty \tag{13}$$

where the factors $R^{s,a}$ are the unknown constants related to R and T by the relation

$$R,\ T = \frac{1}{2}\left(R^s \pm R^a\right)\mathrm{e}^{-2\mathrm{i}Ka} \tag{14}$$

Now, we reduce the boundary-value problem for the velocity potential to a boundary integral equation over Γ_1. To do this, we incorporate an appropriate fundamental solution with an application of Green's integral theorem. We use the fundamental solution

$$\mathfrak{I}(x,y;\xi,\eta) = \log\frac{r}{r'} - 2\int_0^{\infty}\frac{\mathrm{e}^{-k(y+\eta)}}{k-K}\cos k(x-\xi)\,\mathrm{d}k \tag{15}$$

where $r,r' = \left\{\sqrt{(x-\xi)^2 + (y\pm\eta)^2}\right\}$ and $\mathfrak{I}$ satisfies the Eqs. (3) and (4) and has a logarithmic source singularity at the point $(x,y) = (\xi,\eta)$; the path of the integration in the equation (15) is indented below the pole of the integrand at $k = K$. Thus $\mathfrak{I}$ satisfies the radiation condition at infinity.

Now we employ the Green's theorem to the functions

$$\psi^{s,a}(x,y)=\phi^{s,a}(x,y)-\mathrm{e}^{-Ky-\mathrm{i}K(x-a)} \tag{16}$$

and

$$\Im^{s,a}(x,y;\xi,\eta)=\Im(x,y;\xi,\eta)\pm\Im(-x,y;\xi,\eta) \tag{17}$$

in the fluid region bounded externally by the lines

$$y=0,\ 0\le x\le X;\quad x=X,\ 0\le y\le Y$$
$$0\le x\le X,\ y=Y;\quad x=0,\ \ 0\le y\le Y$$

and internally by a small circle of radius ε and centered at (ξ,η) and the contour enclosing the plate Γ_1. We finally make $X,Y\to\infty$ and $\varepsilon\to 0$ and shrink the contour enclosing the plate Γ_1 into both sides of Γ_1 and obtain the integral representation of $\phi^{s,a}(\xi,\eta)$ as

$$\phi^{s,a}(\xi,\eta)=$$
$$2\mathrm{e}^{-Ky+\mathrm{i}Ka}(\cos K\xi,-\mathrm{i}\sin K\xi)-\frac{1}{2\pi}\int_{\Gamma_1}F^{s,a}(q)\frac{\partial\Im^{s,a}}{\partial n_q}\mathrm{d}s_q \tag{18}$$

where $q\equiv(x,\ y)$ is a point on Γ_1, $F^{s,a}(q)$ are the discontinuities of $\phi^{s,a}(x,y)$ across Γ_1 at q and $\dfrac{\partial\Im^{s,a}}{\partial n_q}$ denotes the normal derivative of $\Im^{s,a}$ at the point q. Moreover it should be noted that the unknown functions $F^{s,a}(q)$ vanish at the tips of Γ_1 while their derivatives have square-root singularities there.

Now we finally need to apply the boundary condition on the porous plate surface rewritten as

$$\frac{\partial\phi^{s,a}}{\partial n_p}(\Gamma_1^+)=\frac{\partial\phi^{s,a}}{\partial n_p}(\Gamma_1^-)=-\mathrm{i}KG\left[\phi^{s,a}\right](p) \tag{19}$$

where $p\equiv(\xi,\eta)\in\Gamma_1$. For that purpose we take the normal derivative on the both sides of the Eq. (18) at a point p on Γ_1 and using the boundary condition (19) we get

$$\frac{1}{2\pi}\frac{\partial}{\partial n_p}\int_{\Gamma_1}F^{s,a}(q)\frac{\partial\Im^{s,a}}{\partial n_q}\mathrm{d}s_q=$$
$$\frac{\partial}{\partial n_p}\left[2\mathrm{e}^{-K\eta+\mathrm{i}Ka}(\cos K\xi,-\mathrm{i}\sin K\xi)\right]+\mathrm{i}KGF^{s,a}(p),\ \ p\in\Gamma_1 \tag{20}$$

Eq. (20) is an integra-differential equation in $F^{s,a}(q),\ q\in\Gamma_1$ and is to be solved subject to the condition that

$$F^{s,a}=0 \text{ at the two tips of } \Gamma_1 \tag{21}$$

We now can interchange the order of the integration and the normal differentiation which is legitimate (cf. Martin and Rizzo (1989)) provided that the integral is then to be treated as the Hadamard-finite part integral. By applying this procedure we get

$$\frac{1}{2\pi}\int_{\Gamma_1}F^{s,a}(q)\frac{\partial^2\Im^{s,a}}{\partial n_p\partial n_q}\mathrm{d}s_q-\mathrm{i}KGF^{s,a}(p)=$$
$$\frac{\partial}{\partial n_p}\left[2\mathrm{e}^{-K\eta+\mathrm{i}Ka}(\cos K\xi,-\mathrm{i}\sin K\xi)\right],\ \ p\in\Gamma_1 \tag{22}$$

The integral Eq. (22) is a hypersingular integral equation of the second kind, to be solved subject to the boundary conditions (21). The $\int(\cdot)$ implies that the integral is to be considered as a two-sided finite part integral of order two.

Next, we first convert the kernel of the hypersingular integral equation (22) to a more generalized form. For this purpose we take the unit normals at the points p and q on Γ_1 denoted by n_p and n_q, respectively. Then

$$n_p=(\sin\theta_\tau,-\cos\theta_\tau),\quad n_q=(\sin\theta_t,-\cos\theta_t) \tag{23}$$

where

$$\theta_{t,\tau}=\frac{\alpha+\beta}{2}+\frac{\beta-\alpha}{2}(t,\tau),\quad -1\le t,\ \tau\le 1 \tag{24}$$

and an appropriate parameterization of the curved plate is taken as $x=a+b\sin\theta_t,\ y=d+b(1-\cos\theta_t),\ -1\le t\le 1,$ where $q\equiv(x,y)$.

The point $p\equiv(\xi,\eta)$ on Γ_1 has the same parameterisation, but with t replaced by τ. Using this parameterization we find that

$$\frac{\partial^2\Im^{s,a}}{\partial n_p\partial n_q}=\frac{1}{b^2\Theta^2(t-\tau)^2}+M^{s,a}(\tau,t) \tag{25}$$

where

$$M^{s,a}(\tau,t)=-\frac{1}{4b^2}\left[\frac{1}{\sin^2\dfrac{\Theta}{2}(\tau-t)}-\frac{4}{\Theta^2(\tau-t)^2}\right]-$$
$$\left[\cos(\theta_\tau-\theta_t)\left\{\frac{Y^2-X^2}{\left(X^2+Y^2\right)^2}+\frac{2KY}{X^2+Y^2}+2K^2\Phi_0(X,Y)\right\}+\right.$$
$$2\sin(\theta_\tau-\theta_t)\left\{\frac{XY}{\left(X^2+Y^2\right)^2}+\frac{KX}{X^2+Y^2}+K^2\Omega_0(X,Y)\right\}\mp$$
$$\cos(\theta_\tau-\theta_t)\frac{Z^2-X_1^2}{\left(X_1^2+Z^2\right)^2}\pm\sin(\theta_\tau-\theta_t)\frac{2X_1Z}{\left(X_1^2+Z^2\right)^2}\pm$$
$$\cos(\theta_\tau+\theta_t)\left\{\frac{Y^2-X_1^2}{\left(X_1^2+Y^2\right)^2}+\frac{2KY}{X_1^2+Y^2}+2K^2\Phi_0(X_1,Y)\right\}\mp$$
$$\left.2\sin(\theta_\tau+\theta_t)\left\{\frac{X_1Y}{\left(X_1^2+Y^2\right)^2}+\frac{KX_1}{X_1^2+Y^2}+K^2\Omega_0(X_1,Y)\right\}\right] \tag{26}$$

with

$$\begin{gathered} X = x-\xi = b(\sin\theta_t - \sin\theta_\tau) \\ Y = y+\eta = 2(d+b) - b(\cos\theta_t + \cos\theta_\tau) \\ X_1 = x+\xi = 2a + b(\sin\theta_t + \sin\theta_\tau) \\ Z = y-\eta = b(\cos\theta_t - \cos\theta_\tau) \\ \Theta = \frac{1}{2}(\beta-\alpha) \\ \Phi_0(X,Y),\ \Omega_0(X,Y) = \int_0^\infty \frac{\mathrm{e}^{-KY}}{k-K}(\cos kX, \sin kX)\,\mathrm{d}k \end{gathered} \tag{27}$$

The right hand side of the Eq. (22) can be expressed as

$$\frac{\partial}{\partial n_p}\left[2\mathrm{e}^{-K\eta+\mathrm{i}Ka}(\cos K\xi, -\mathrm{i}\sin K\xi)\right] = h_1^{s,a}(\tau)$$

where

$$h_1^{s,a}(\tau) = 2K\mathrm{e}^{-K\eta+\mathrm{i}Ka}\{\cos(K\xi+\theta_\tau), -\mathrm{i}\sin(K\xi+\theta_\tau)\} \tag{28}$$

Now the Eq. (22) can finally be rewritten as

$$\begin{gathered} \int_{-1}^{1} f^{s,a}(t)\left[-\frac{1}{(t-\tau)^2} + b^2\Theta^2 M^{s,a}(\tau,t)\right]\mathrm{d}t - \\ \mathrm{i}Kb\Theta G f^{s,a}(\tau) = h^{s,a}(\tau), \quad -1<\tau<1 \end{gathered} \tag{29}$$

where

$$h^{s,a}(\tau) = 2\pi b\Theta h_1^{s,a}(\tau) \tag{30}$$

and $f^{s,a}(t)$ stands for $F^{s,a}(q)$. If $G=0$, the Eq. (29) reduces to a first kind hypersingular integral equation (cf. Mandal and Gayen (2002)) as follows

$$\int_{-1}^{1} f^{s,a}(t)\left[-\frac{1}{(t-\tau)^2} + b^2\Theta^2 M^{s,a}(\tau,t)\right]\mathrm{d}t = h^{s,a}(\tau), \quad -1<\tau<1$$

The hypersingular integral Eq. (29) are to be solved subject to the end condition that $f^{s,a}=0$.

Now, using the method of contour integration the integrals in (26) can be expressed as

$$\begin{gathered} \Phi_0(X,Y) = \int_0^\infty \frac{\mathrm{e}^{-KY}}{k-K}(\cos kX)\,\mathrm{d}k = \\ \pi\mathrm{i}e^{-KY+\mathrm{i}K|X|} - \int_0^\infty \frac{K\sin kY - k\cos kY}{k^2+K^2}\mathrm{e}^{-K|X|}\mathrm{d}k \\ \Omega_0(X,Y) = \int_0^\infty \frac{\mathrm{e}^{-KY}}{k-K}(\sin kX)\mathrm{d}k = \\ \pi\mathrm{e}^{-KY+\mathrm{i}K|X|} - \int_0^\infty \frac{K\cos kY + k\sin kY}{k^2+K^2}\mathrm{e}^{-K|X|}\mathrm{d}k \end{gathered}$$

Now to solve the Eq. (29), we begin with approximating the unknown functions $f^{s,a}(t)$ in the following way (cf. Gayen and Mondal (2014)). Let

$$f^{s,a}(t) \cong \sqrt{1-t^2}\sum_{n=0}^{N} a_n^{s,a} U_n(t) \tag{31}$$

where $U_n(t)$ is the Chebyshev polynomial of the second kind and the unknown factors, a_n's are to be determined. The square-root factor in (31) ensures that $f^{s,a}(t)$ have the right behavior at each tip of the plates, where the potential difference vanishes. Substituting the expansion (31) in the place of all $f^{s,a}(t)$ in (29) we finally get

$$\sum_{n=0}^{N} a_n^{s,a} A_n^{s,a}(\tau) = h_n^{s,a}(\tau), \quad -1<\tau<1 \tag{32}$$

where

$$\begin{gathered} A_n^{s,a}(\tau) = \pi(n+1)U_n(\tau) + \\ \int_{-1}^{1} b^2\Theta^2\sqrt{1-t^2}M^{s,a}(\tau,t)U_n(t)\mathrm{d}t - 2\pi\mathrm{i}Kb\Theta G\sqrt{1-\tau^2}U_n(\tau) \end{gathered} \tag{33}$$

Next, we collocate at $\tau=\tau_j$, $j=0,1,...,N$, where τ_j's are chosen as

$$\tau_j = \cos\left(\frac{(2j+1)\pi}{2N+2}\right), \quad j=0,1,...,N \tag{34}$$

these being the zeros of $T_{n+1}(\tau)$, the Chebyshev polynomial of the first kind. Golberg (1983; 1985) has shown that the Eq. (34) is a good choice since it provides a uniform convergent method. The rate of convergence of his method depends on the smoothness of the kernel $M^{s,a}$ in the Eq. (29).

The two linear systems of equations which are formed by replacing τ with τ_j in the equation (32) are now to be solved numerically by applying any standard method.

1) Reflection and transmission coefficients.

From the Eq. (14) it is evident that to determine $|R|$ and $|T|$ we first have to compute the unknown quantities $R^{s,a}$. We first make $\xi\to\infty$ in the representation of $\phi^{s,a}(\xi,\eta)$ as given in Eq. (18) and then compare it with (13) (with (x, y) replaced by (ξ,η)). Also we need to make use of the asymptotic results

$$\mathfrak{I}^{s,a}(x,y;\xi,\eta) \to -4\pi\mathrm{e}^{-K(y+\eta)+\mathrm{i}K\xi}(\mathrm{i}\cos Kx, -\sin Kx) \text{ as } \xi\to\infty \tag{35}$$

Finally we find that

$$\begin{gathered} R^{s,a} = \pm\mathrm{e}^{2\mathrm{i}Ka} + 2\mathrm{e}^{\mathrm{i}Ka}\int_{\Gamma_1} F^{s,a}(q)\frac{\partial}{\partial n_q}\left[\mathrm{e}^{-Ky}(\mathrm{i}\cos Kx, \sin Kx)\right]\mathrm{d}s_q = \\ \pm\mathrm{e}^{2\mathrm{i}Ka} + 2Kb\Theta\mathrm{e}^{\mathrm{i}Ka}\sum_{n=0}^{N} a_n^{s,a}\int_{-1}^{1}\sqrt{1-t^2}U_n(t)\mathrm{e}^{-K\{d+b(1-\cos\theta_t)\}}\times \\ \{\mathrm{i}\cos(Ka+Kb\sin\theta_t+\theta_t), \sin(Ka+Kb\sin\theta_t+\theta_t)\}\mathrm{d}t \end{gathered} \tag{36}$$

Thus, once we get the numerical estimates of $R^{s,a}$ by solving the integrals in Eq. (36), R and T can be computed using the Eq. (14). We have depicted the results for R and T in a number of figures in section 4.

2) Hydrodynamic forces on the plates.

The hydrodynamic forces acting on each curved porous plate can be determined as follows:

The fluid pressure $p(x,y,t')$ at a point (x, y) is connected to the velocity potential $\Phi(x,y,t')$ by the expression

$$p(x,y,t') = \rho\frac{\partial \Phi}{\partial t}(x,y,t') + \rho g y \tag{37}$$

where $\Phi(x,y,t') = \mathrm{Re}\left\{\frac{g^2}{\sigma^3}\phi(x,y)\mathrm{e}^{-\mathrm{i}\sigma t'}\right\}$ and ρ is the water density. Therefore the force per unit width of each plate Γ_i, $i = 1,2$ can be expressed as

$$H_i = \frac{\rho g}{K}\int_{\Gamma_i}\mathrm{Re}\left\{\mathrm{i}\left(\phi^+ - \phi^-\right)(q)\mathrm{e}^{-\mathrm{i}\sigma t'}\right\}\mathrm{d}s_q \tag{38}$$

where q is a point on the plate Γ_i. Using the parametric coordinates of q, the dimensionless forces acting on the curved porous plates can be expressed as

$$\mathcal{H}_1 = \left|\frac{KH_1}{\rho g b}\right| = \left|\int_{\Gamma_1}\mathrm{Re}\left\{\mathrm{i}\left(f^s(t) + f^a(t)\right)\mathrm{e}^{-\mathrm{i}\sigma t'}\right\}\Theta\mathrm{d}t\right| \tag{39}$$

and

$$\mathcal{H}_2 = \left|\frac{KH_2}{\rho g b}\right| = \left|\int_{\Gamma_2}\mathrm{Re}\left\{\mathrm{i}\left(f^s(t) - f^a(t)\right)\mathrm{e}^{-\mathrm{i}\sigma t'}\right\}\Theta\mathrm{d}t\right| \tag{40}$$

The numerical estimates for these quantities can be evaluated using the solutions of the hypersingular integral Eq. (29).

4 Numerical results

In this section we will discuss the effect of different parameters i.e. arc-length, porosity, depth *etc*. on the reflection and the transmission coefficients and the hydrodynamic forces acting on the porous plates. We have made different physical quantities dimensionless with respect to the radius *b*. While taking the values of $|R|$, $|T|$ it has always been verified that the computed values of these two quantities are always satisfied by the following energy identities

$$|R|^2 + |T|^2 = 1 \quad \text{for} \quad G = 0 \tag{41}$$

and

$$|R|^2 + |T|^2 = 1 - J \quad \text{for} \quad G \neq 0 \tag{42}$$

where

$$J = \frac{1}{2}KbG_r\Theta\left[\int_{-1}^{1}|f^s(t) + f^a(t)|^2\,\mathrm{d}t + \int_{-1}^{1}|f^s(t) - f^a(t)|^2\,\mathrm{d}t\right] \tag{43}$$

This will give a partial check on the correctness of the numerical results obtained here.

To validate our numerical results, we present Table 1. In this table, the numerical estimates for $|R|$ and $|T|$ are presented for $\alpha = 30°$, β=180°, $d/b = 0.5$, $G = 1$, $a/b = 1.5$ against the wave number *Kb*. We have computed these values using Eq. (36) together with Eq. (14) and have presented $|R|^2 + |T|^2$ in the fourth column of Table 1. The quantity $1 - J$ has been computed from Eq. (43) using the solutions $f^{s,a}(t)$ of the hypersingular integral Eq. (29). Comparing the values in the fourth and fifth columns it is clearly visible that $|R|$ and $|T|$ satisfy the energy balance relation (42).

Table 1 Reflection and the transmission coefficients

Kb	$\|R\|$	$\|T\|$	$\|R\|^2 + \|T\|^2$	$1 - J$
0.3	0.030 6	0.846 7	0.717 8	0.717 8
0.6	0.151 1	0.782 3	0.634 8	0.634 8
0.9	0.115 5	0.814 6	0.677 0	0.677 0
1.2	0.045 6	0.859 5	0.740 8	0.741 1
1.5	0.065 3	0.891 0	0.798 2	0.798 8

Fig. 2 illustrates $|R|$ against the dimensionless wave number *Kb* for two semi circular porous plates. Here we have taken the values of different parameters as $\alpha = 0$, $\beta = \pi$, $d/b = 0.5$, $G = 1$. Graphs have been plotted for two different values of the length of separation a/b(1.5, 1.0). Fig. 2 shows that for larger frequencies of the wave, an increase in the distance between the plates causes more reflection. This happens because the scope of multiple reflections between the plates increases as the length of separation between them increases. As a result the overall reflection increases.

Fig. 3 stands for a comparison in the reflective and transmissive properties between the systems of two closely placed semi-circular arc-shaped plates: one consists of two permeable plates and the other consists of two impermeable plates. Such a configuration serves almost as the cross section of a horizontal circular cylinder. It is observed that for both the cases (*G*=0 or 1) the amount of reflection is very low. This is consistent with the phenomenon of zero reflection by a horizontal circular cylinder. This result was established long ago by Ursell (1950) for a rigid horizontal cylinder and was verified by Mandal and Gayen (2002) by taking two semi-circular rigid plates whose vertical diameters are very close to each other. The solid line represents the data of Mandal and Gayen (2002), and the dashed line in the curve of reflection coefficient stands for the results obtained by the present method. It can be seen that a horizontal porous cylinder also offers no hindrance to

the propagation of water waves. The reflection as well as the transmission for the porous cylinder is even less than that for a rigid one.

In Fig. 4, the effect of different arc-lengths of the porous plates on $|R|, |T|$ is depicted against Kb for fixed values of the depth parameter $d/b(0.5)$, separation constant $a/b(1.5)$ and porous effect parameter G=1. Here the graphs have been drawn for three different values of the arc lengths of the porous plates ($\alpha = 30°, \beta = 180°, 120°, 90°$). The occurrence of zeros of $|R|$ as a function of wave number is one of the most important features. From Fig. 4 it is observed that the zeros of $|R|$ are shifted towards the right with the decrease in the arc length of the plates. Also, $|R|$ decreases with the decrease in arc-length due to the fact that the incident wave train faces less hindrance with the decrease in arc-length. For the case of transmission, $|T|$ decreases with the increase in arc-length. Moreover, in this figure, the multiple peaks appear due to multiple reflections by the edges of the two plates. Whenever a system of breakwaters comprising of more than one barrier is present, such reflection is obvious. As a reference, we may mention the work of Karmakar and Soares (2014) who considered a system of bottom standing porous plates where the reflection curves also have multiple peaks (Figs. 3–9, Page. 55–58).

Fig. 5 displays the variation of $|R|$ for the systems of two circular arc shaped impermeable plates (G=0) and two circular arc shaped permeable (G=1) plates for fixed arc-lengths of the plates. These two figures have been plotted for $a/b = 1.5, \alpha = 5°, \beta = 150°$. From Fig. 5 it may be seen that as the depth of the upper end of the plates from the free surface decreases, the value of $|R|$ increases i.e. more wave energy is reflected back by the plates. This happens because the disturbance created by the incident wave train cannot penetrate much below the free surface and as a result less wave energy is reflected back by the plate whose depth from the free surface is significant. The main difference between these graphs is that the heights of the reflection curves are less for permeable plates (G=1) than impermeable plates (G=0). Therefore less energy is reflected by the porous structures. Also the the graphs for G=0 have a very good agreement with the corresponding results obtained by Mandal and Gayen (2002) for two circular arc shaped rigid barriers.

In Fig. 6, the effect of porosity on the dissipated energy has been shown graphically for $d/b = 0.5, a/b = 1.5, \alpha = 30°, \beta = 90°$. From this figure it is clear that for Kb<0.45, energy dissipation increases with the increase in the porous-effect parameter G. However, for larger wave numbers, the reverse phenomenon occurs.

Fig. 7 describes the results for two submerged almost full circles i.e. two circular cylinders. Here $|R|$ and $|T|$ have been plotted against Kb for $d/b = 0.5, a/b = 1.5, \alpha = 0°, \beta = 359°$. We have also checked for other sets of values of α, β for which we get two almost full circles (e.g. $\alpha = -60°, \beta = 299°$) and got almost the same curves. It may be observed from this figure that as the value of the porous-effect-parameter G increases the incoming waves experience less reflection and less transmission. For the case $G = 1$ there is almost no reflection. This happens since some part of the wave energy is dissipated on the surface of the porous plates due to the internal friction. This phenomenon is very important in coastal engineering, because porous structures cause smaller surface fluctuation due to the low reflection, which is important for ship loading and unloading.

The effect of transition, from a circular-arc-shaped plate which is symmetric about the vertical, to an almost horizontal plate of same arc-length on the reflection and the transmission coefficients, can be seen in Fig. 8 by making the separation length (a/l) zero where 2l is the constant arc-length of the plate. Here $|R|$ and $|T|$ have been plotted against a new wave number Kl. The graphs have been plotted for $d/l = 0.1, \alpha = 0°$ and $\beta = 36°$ when $l = b\beta$ has been kept fixed. The characteristics of the curve for $|R|$ due to switching from a circular-arc-shaped plate to a nearly horizontal plate are observed to be the same as given by Mandal and Gayen (2002). The fact that a porous nearly horizontal plate system is more transparent to the incident wave compared to a rigid nearly horizontal plate system is also visible here. Also from this figure it is clear that for permeable plates the transmission coefficient decreases rapidly with the wave number.

In Figs. 9 and 10 the dimensionless amplitudes of the hydrodynamic forces acting on the plates have been plotted against non-dimensional wave number Kb by taking $d/b = 0.5, a/b = 1, \alpha = 0°, \beta = 180°, t' = 0$. Here the graphs have been drawn for three different values of the porous effect parameter G (G=1, 1.5, 2). If the graphs of these figures are compared, we can see that less force is experienced by the rear plate compared to the front plate. Also, the magnitude of the hydrodynamic forces acting on the plate decreases with the increase in porosity of the plate. It may also be noticed from Fig. 10 that the force curves are somewhat oscillatory in nature for the plate Γ_2 due to the presence of the four plate tips. It first increases with Kb, attains zero value and then gradually increases again.

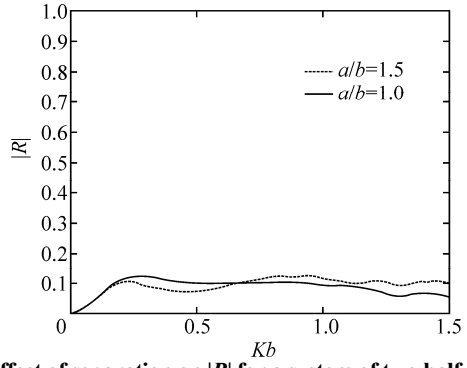

Fig. 2 Effect of separation on $|R|$ for a system of two half-circular porous plates ($\alpha = 0$, $\beta = \pi$, $d/b = 0.5$, $G = 1$)

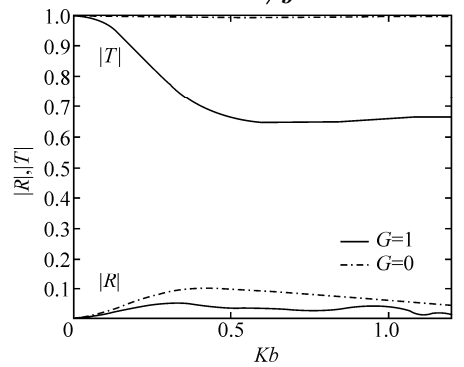

Fig. 3 Reflection and transmission coefficients for two half-circular impermeable and permeable plates ($\alpha = 0$, $\beta = \pi$, $d/b = 0.5$, $a/b = 0.001$)

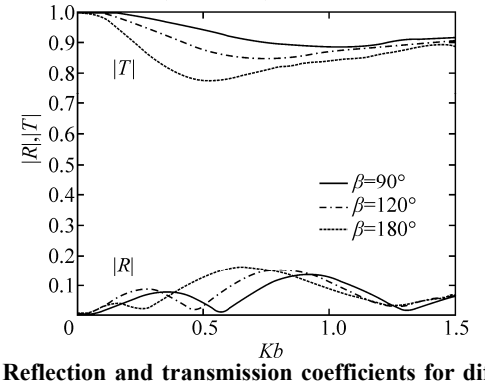

Fig. 4 Reflection and transmission coefficients for different arc-lengths of two curved porous plates ($a/b = 1.5$, $d/b = 0.5$, $G = 1$, $\alpha = 30°$)

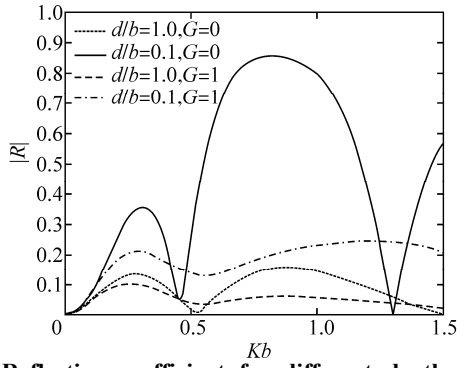

Fig. 5 Reflection coefficient for different depths of two permeable and impermeable curved plates ($a/b = 1.5$, $G = 0$, $\alpha = 5°$, $\beta = 150°$)

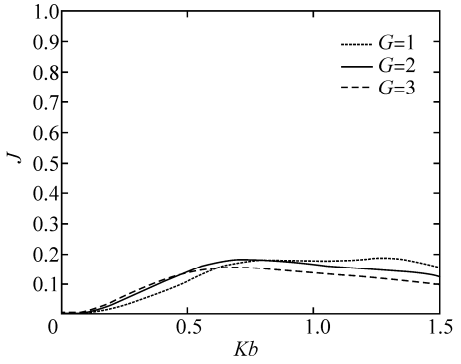

Fig. 6 Dissipated energy for two curved porous plates, for various G ($d/b = 0.5$, $a/b = 1.5$, $\alpha = 30°$, $\beta = 90°$)

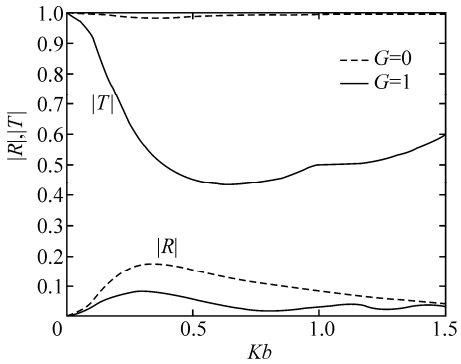

Fig. 7 Reflection and transmission coefficients for two almost full circles ($d/b = 0.5$, $a/b = 1.5$, $\alpha = 0°$, $\beta = 359°$)

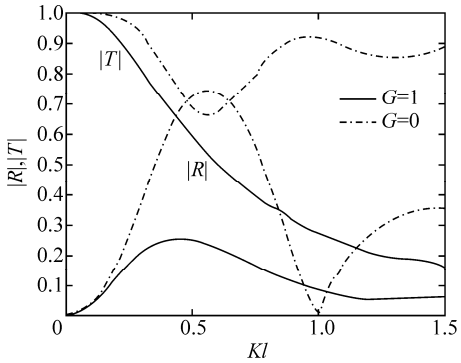

Fig. 8 Reflection and transmission coefficient for small $\beta - \alpha$ ($d/l = 0.1$, $a/l = 0$, $\alpha = 0°$, $\beta = 36°$, $G = 0$, 1)

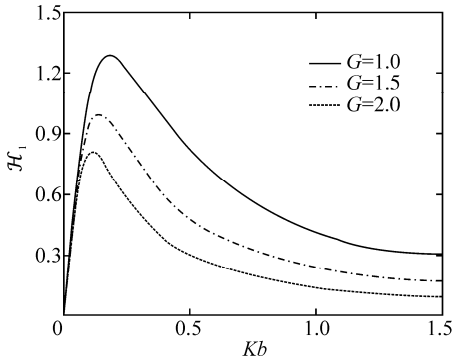

Fig. 9 Amplitude of the hydrodynamic forces acting on Γ_1 ($d/b = 0.5$, $a/b = 1$, $\alpha = 0°$, $\beta = 180°$)

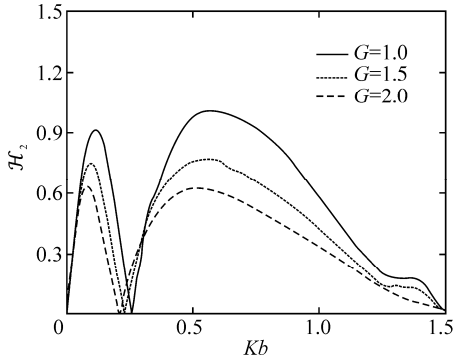

Fig. 10 Amplitude of the hydrodynamic forces acting on Γ_2 ($d/b = 0.5$, $a/b = 1$, $\alpha = 0°$, $\beta = 180°$)

5 Conclusions

The problem of water wave scattering by two symmetric circular-arc-shaped porous plates submerged in deep water has been discussed with linear theory. The plates are situated symmetrically about vertical lines passing through the midpoint of the line joining the centers of circles whose arcs are assumed to be the positions of the plates. Exploiting the geometrical symmetry of the plates, the velocity potential has been divided into its symmetric and anti-symmetric parts. Appropriate use of Green's integral theorem to the suitable functions in the fluid region, followed by the utilization of the boundary condition on the porous plate surface, yielded two hypersingular integral equations of the second kind. These are solved using an expansion-collocation method. Using the numerical solutions of these hypersingular integral equations, the reflection and the transmission coefficients and the hydrodynamic forces on the plates have been determined and depicted graphically in a number of figures. The numerical results for the reflection coefficient for two circular-arc-shaped rigid barriers have been obtained as a special case and matched with the corresponding published paper of Mandal and Gayen (2002). A good agreement has been achieved. After analyzing the numerical results for the reflection coefficient obtained here, it may be concluded that the incoming waves experience less reflection due to the presence of the dual plates system consisting of two curved porous plates compared to that consisting of two similar rigid plates. Thus a dual circular plate system provides an effective model for porous barriers, as the system effectively reduces the height of the reflected wave, which is useful in reducing the occurrence of wave resonance inside harbours. It is also established that, like a rigid horizontal circular cylinder, a porous horizontal cylinder is also transparent to the incoming waves.

References

Das P, Dolai DP, Mandal BN (1997). Oblique wave diffraction by parallel thin vertical barriers with gaps. *Journal of Waterway, Port, Coastal, and Ocean Engineering*, **123**(4), 163-171. DOI: 10.1061/(ASCE)0733-950X(1997)123:4(163)

De SM, Mandal BN, Chakrabarti A (2009). Water-wave scattering by two submerged plane vertical barriers—Abel integral-equation approach. *Journal of Engineering Mathematics*, **65**(1), 75-87. DOI: 10.1007/s10665-009-9265-3

De SM, Mandal BN, Chakrabarti A (2010). Use of Abel integral equations in water wave scattering by two surface-piercing barriers. *Wave Motion*, **47**(5), 279-288. DOI: 10.1016/j.wavemoti.2009.12.002

Evans DV (1970). Diffraction of water waves by a submerged vertical plate. *Journal of Fluid Mechanics*, **40**(3), 433-451. DOI: 10.1017/S0022112070000253

Gayen R, Mondal A (2014). A hypersingular integral equation approach to the porous plate problem. *Applied Ocean Research*, **46**, 70-78. DOI: 10.1016/j.apor.2014.01.006

Golberg MA (1983). The convergence of several algorithms for solving integral equations with finite-part integrals. *Journal of Integral Equations*, **5**, 329-340.

Golberg MA (1985). The convergence of several algorithms for solving integral equations with finite-part integrals II. *Journal of Integral Equations*, **9**, 267-275.

Isaacson M, Baldwin J, Premasiri S, Yang G (1999). Wave interactions with double slotted barriers. *Applied Ocean Research*, **21**(2), 81-91. DOI: 10.1016/S0141-1187(98)00039-X

Jarvis RJ (1971). The scattering of surface waves by two vertical plane barriers. *Journal of the Institute of Mathematics and its Applications*, **7**, 207-215.

Kanoria M, Mandal BN (2002). Water wave scattering by a submerged circular-arc-shaped plate. *Fluid Dynamics Research*, **31**(5-6), 317-331. DOI: 10.1016/S0169-5983(02)00136-3

Karmakar D, Guedes Soares C (2014). Wave transformation due to multiple bottom-standing porous barriers. *Ocean Engineering*, **80**, 50-63 DOI: 10.1016/j.oceaneng.2014.01.012

Koraim AS, Heikal EM, Rageh OS (2011). Hydrodynamic characteristics of double permeable breakwater under regular waves. *Marine Structures*, **24**(4), 503-527. DOI: 10.1016/j.marstruc.2011.06.004

Levine H, Rodemich E (1958). *Scattering of surface waves on an ideal fluid*. Mathematics and Statistics Laboratory, Stanford University, Palo Alto, USA, Technical Report No.78.

Losada IJ, Losada MA, Roldán AJ (1992). Propagation of oblique incident waves past rigid vertical thin barriers. *Applied Ocean Research*, **14**(3), 191-199. DOI: 10.1016/0141-1187(92)90014-B

Lu CJ, He YS (1989). Reflexion and transmission of water waves by a thin curved permeable barrier. *Journal of Hydrodynamics*, **1**(3), 77-85.

Mandal BN, Chakrabarti A (2000). *Water wave scattering by barriers*. WIT Press, Southampton, UK.

Mandal BN, Gayen R (2002). Water-wave scattering by two symmetric circular-arc-shaped thin plates. *Journal of Engineering Mathematics*, **44**(3), 297-309. DOI: 10.1023/A:1020944518573

Martin PA, Rizzo FJ (1989). On boundary integral equations for crack problems. *Proceedings of the Royal Society of London, Series A: Mathematical and Physical Sciences*, **421**(1861), 341-355. DOI: 10.1098/rspa.1989.0014

McIver M, Urka U (1995). Wave scattering by circular arc shaped plates. *Journal of Engineering Mathematics*, **29**(6), 575-589. DOI: 10.1007/BF00044123

Neelamani S, Vedagiri M (2002). Wave interaction with partially immersed twin vertical barriers. *Ocean Engineering*, **29**(2), 215-238. DOI: 10.1016/S0029-8018(00)00061-5

Newman JN (1974). Interaction of water waves with two closely spaced vertical obstacles. *Journal of Fluid Mechanics*, **66**(1), 97-106. DOI: 10.1017/S0022112074000085

Twu SW, Lin DT (1991). On a highly effective wave absorber. *Coastal Engineering*, **15**(4), 389-405. DOI: 10.1016/0378-3839(91)90018-C

Parsons NF, Martin PA (1994). Scattering of water waves by submerged curved plates and by surface-piercing flat plates. *Applied Ocean Research*, **16**(3), 129-139. DOI: 10.1016/0141-1187(94)90024-8

Porter D (1972). The transmission of surface waves through a gap in a vertical barrier. *Mathematical Proceedings of the Cambridge Philosophical Society*, **71**(2), 411-421. DOI: 10.1017/S0305004100050647

Ursell F (1947). The effect of a fixed vertical barrier on surface waves in deep water. *Mathematical Proceedings of the Cambridge Philosophical Society*, **43**(3), 374-382. DOI: 10.1017/S0305004100023604

Ursell F (1950). Surface waves on deep water in the presence of a submerged circular cylinder. I. *Mathematical Proceedings of the Cambridge Philosophical Society*, **46**(1), 141-152. DOI: 10.1017/S0305004100025561

Yu XP, Chwang AT (1994). Wave-induced oscillation in harbor with porous breakwaters. *Journal of Waterway, Port, Coastal, and Ocean Engineering*, **120**(2), 125-144. DOI: 10.1061/(ASCE)0733-950X(1994)120:2(125)

The 12th International Conference on Hydrodynamics (ICHD 2016)

September 18–23, 2016
Delft, The Netherlands

Hydrodynamics has always been an important and fundamental subject for many disciplines involving the science of forces acting on or exerted by fluids, and engineering applications including ship and marine engineering, ocean and coastal engineering, mechanical and industrial engineering, environmental engineering, hydraulic engineering, petroleum engineering, biological & biomedical engineering, and so on.

While many engineering questions have been answered, there are still many more that need to be addressed through field trial, verification and fundamental research and development (R&D). The International Conference on Hydrodynamics (ICHD) is the forum for participants from around the world to review, discuss and present the latest developments in the broad discipline of hydrodynamics and fluid mechanics.

The first International Conference on Hydrodynamics (ICHD) was initiated in 1994 in Wuxi, China. Since then, 11 more ICHD conferences were held in Hong Kong, Seoul, Yokohama, Tainan, Perth, Ischia, Nantes, Shanghai, St Petersburg and Singapore. Evidently the ICHD conference has become an important event among academics, researchers, engineers and operators, working in the fields closely related to the science and technology of hydrodynamics.

The scope of the Conference will be broad, covering all the aspects of theoretical and applied hydrodynamics. Specific topics include, but are not limited to:

- Linear and non-linear waves and current
- Ship hydrodynamics resistance, propulsion, powering, seakeeping, manoeuvrability, slamming, sloshing, impact, green water
- Cavitation and cavitating flows
- Hydrodynamics in ocean, coastal and estuary engineering
- Fluid-structural interactions and hydroelasticity
- Hydrodynamics in hydraulic engineering
- Industrial fluid dynamics
- Computational fluid dynamics
- Ocean and atmosphere dynamics
- Environmental hydrodynamics
- Advanced experimental techniques
- Multiphase flow
- Theoretical hydrodynamics
- Bio fluid mechanics

Contact
ICHD2016 Conference Secretariat
Monique Gazendam, tel +31 15 2789714
Dineke Heersma, tel +31 15 2785621
Email: secr-mtt-3me@tudelft.nl

Website: http://www.ichd-home.com